D4.1 Report on Andreev level spin transitions

Author	Affiliation	Email
Christian Schönenberger	UBAS	Christian.Schoenenberger@unibas.ch
Project Number	Project Start Date	Duration
828948	01.04.2019	48 Months
Classification		
	PU	
File Name		
AndQC_deliverable_4.1.docx		
WP No	Work Package Name	
4	WP4 - The Andreev spin qubit (UBAS, BME, CEA, Chalmers, UAM)	
Deliverable No	Deliverable Name	
1	Coupling of microwaves to the Andreev spin (UniBAS, CEA, UAM, Chalmers):	
	Approved by	
	Steering Committee of the action	

The opinions expressed in the document are of the authors only and no way reflect the European Commission's opinions. The European Union is not liable for any use that may be made of the information. This project has received funding from the European Union's Horizon 2020 research and innovation programme under grant agreement No 828948.

DOCUMENT REVISION HISTORY

Revision	Date	Description	Author
1.0	25.9.2021	AndQC_deliverable_4.1_V1.docx	C. Schönenberger
2.0	29.9.2021	AndQC_deliverable_4.1_V2.docx	A. Levy-Yeyati and M. Goffman
3.0	29.92021	AndQC_deliverable_4.1_V3.docx	C. Schönenberger (finalized references)

Table of Contents

1. **Introduction**

Deliverable 4.1 describes the outcome of task 4.1 within work package 4 on spinful Andreev level transitions, of which the basis states of the Andreev spin qubit (ASQ) are constructed. The task description reads: *"Coupling of microwaves to the Andreev spin: The basis of qubit manipulation is the coupling between microwave photons and the spin transition. The purpose of this task is to map this transition in the presence of a weak magnetic field, spin-orbit coupling and multiple propagating modes."*

In the past four years, the following has been achieved, a large fraction by institutions that are partners within AndQC: The coupling of microwaves to the Andreev spin in the presence of strong spin-orbit interaction has been investigated in Josephson junctions (JJs) made from in-situ Al-coated InAs nanowires (NWs) by the CEA, UAM and Chalmers team. The InAs NWs have been delivered by UCPH. For the first time, spin-resolved Andreev states could be addressed both in dispersive measurements of the JJ coupled inductively to a microwave resonator and in excitation spectroscopy applying two-tone spectroscopy. The UAM theory group together with the CEA team have been successful in describing the experiments and made important predictions that could be confirmed in practice. Lastly, coherent control of the Andreev spin qubit with microwave photons has been demonstrated very recently by a collaboration between the group of M. Devoret at Yale and AndQC partners from UCPH, UAM and Chalmers. Since the task has been accomplished with all essential results appeared in publications, we only provide here a short review to guide the reader to the respective publications.

2. **Circuit QED approach to explore Andreev states with microwave photons**

CEA has already several years of experience in coupling few-mode JJs to on-chip superconducting microwave resonators. As material system, the CEA team has been studying single atom junctions in depth. Here, one can tune the junction to a single transport channel with high transmission. Since this is difficult to achieve in other platforms, the atomic-point contact work serves as a reference.[1-5] Within AndQC, the CEA, Chalmers and UBAS team realized JJs made from InAs NWs with strong spin orbit interaction (SOI), which were provided by UCPH, embedded in an RF loop inductively coupled to a microwave resonator. Two kind of InAs-based JJ were used: JJs obtained by direct shadowing of the semiconductor during the in-situ deposition of Al (UBAS)and JJs obtaining by wet etching of a short section of core-shell Al-InAs NWs (CEA). Figure 1 shows a typical device of the first type whereas Fig. 2 shows a device of the second type.

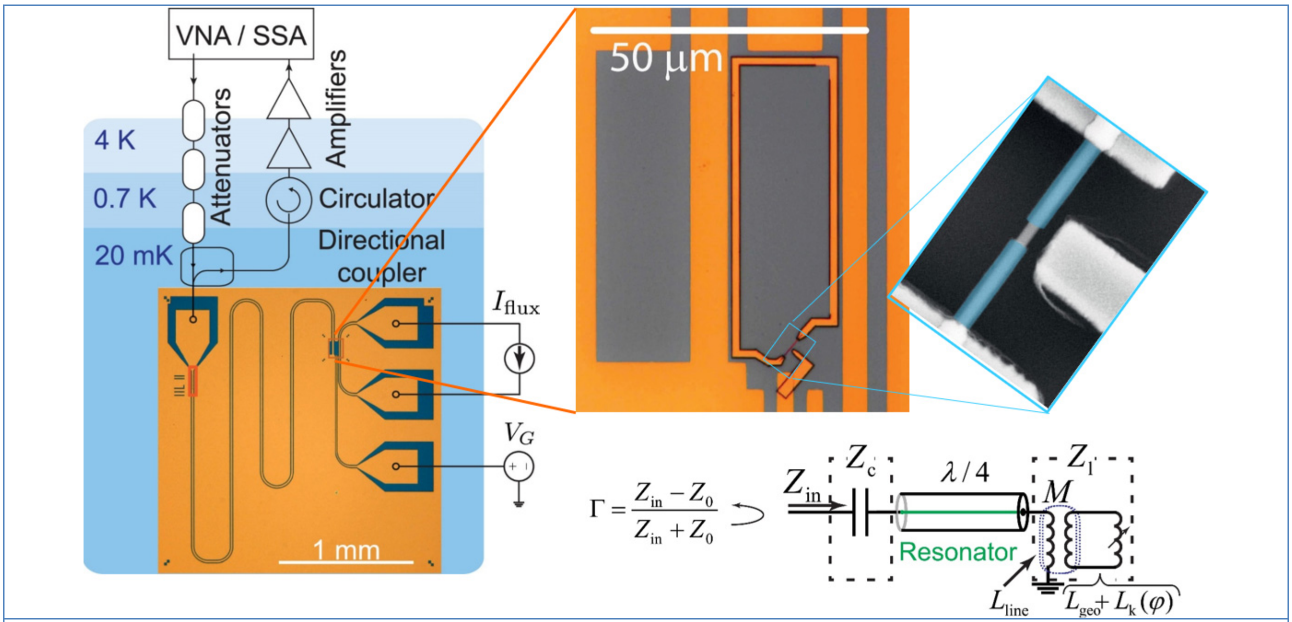

Fig. 1: InAs Nanowire Josephson Junction coupled to a Microwave Resonator *Example from UBAS showing an earlier device layout. The nanowire is embedded in a loop that is inductively coupled to the end of the* $\lambda/4$ *superconducting resonator made from magnetic-field resilient NbTiN. The resonator is probed in reflection.*[6]

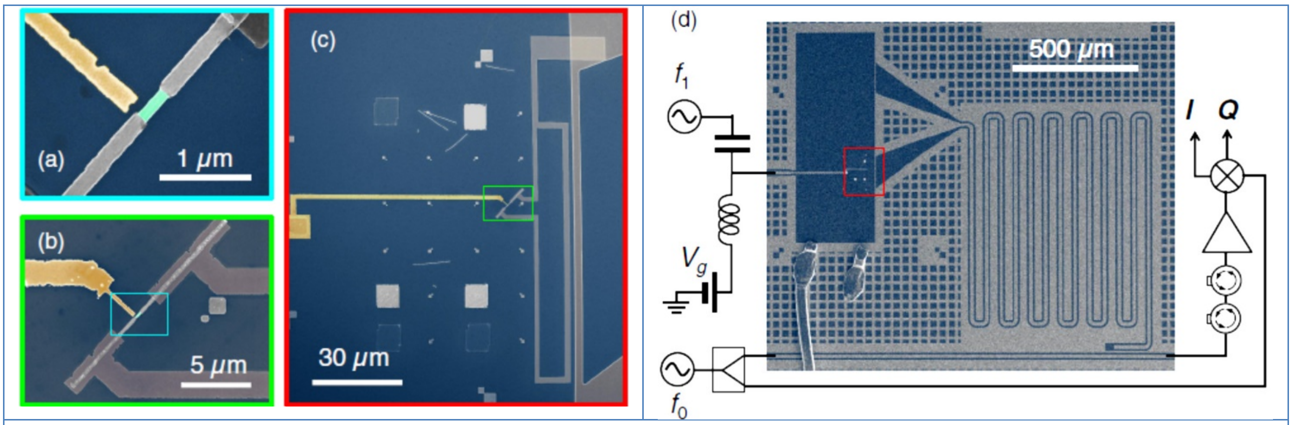

__Fig. 2: InAs Nanowire Josephson Junction coupled to a Microwave Resonator__ Example by CEA taken from Tosi et al. [7] *In this example, a bias tee at the sidegate allows coupling a high-frequency tone $\boldsymbol{f_1}$ to the gate. This is used for two-tone spectroscopy where $\boldsymbol{f_1}$ is varied while the response of the resonator is measured with a fixed tone $\boldsymbol{f_0}$ close to the (bare) resonance frequency. This is done by measuring both the in- and out-of-phase components of the signal transmission through the feedline seen at the bottom. If $\boldsymbol{f_1}$ corresponds to a transition energy, the population distribution is changed. This results in a measurable shift the frequency of the resonator.*

Figure 3 shows the effective circuit as a schematic.[8] The goal of work package 4 is to demonstrate, a) the possibility to lift the spin degeneracy of the Andreev states, which are normally doublets, b) to measure the split states within a circuit-QED approach where a microwave resonator is used as readout device and c) to control spin-state populations and realize coherent manipulation (the latter is part of tasks 4.2 and 4.3).

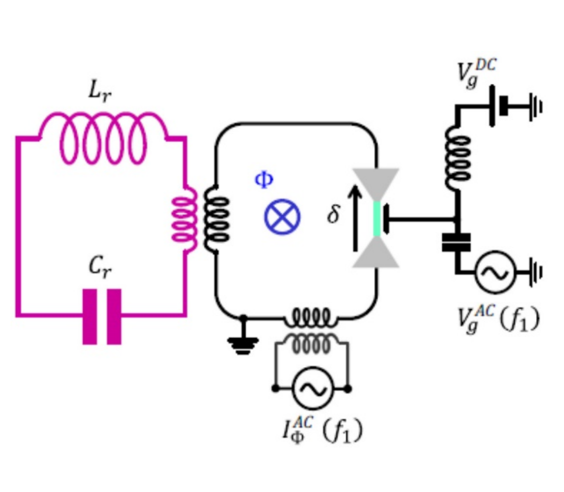

__Fig. 3: Effective Circuit Diagram__ taken from Metzger et al. [8] *The resonator is shown as an LC circuit in magenta on the left side. It is inductively coupled to the RF-SQUID loop in which the nanowire JJ is embedded. A flux through the loop imposes a phase bias $\boldsymbol{\delta}$. Since the junction is made from a semiconducting material carriers-density and subband occupation can be tuned by an electrical field applied to the side gate, seen on the right. The schematics also indicates the two coupling schemes for two-tone spectroscopy: a) through a gate voltage or b) through an induced AC current. The latter couples to spin states if spin-split Andreev levels with odd occupation carry different supercurrents. The former requires SOI which couples spin with charge.*

There have been theoretical and experimental studies before the start of the AndQC project on how a JJ weak-link affects a resonator. A particular important example is the atomic point contact,[9] where the weak-link is defined in the short-junction limit by a single Andreev bound state and with a widely tunable transparency [1-4]. And quite on the opposite scale, are short and long SNS junctions in metallic diffusive wires with many transport channels. Here detailed (linear) response functions have been derived [10-12] with the understanding that the imaginary part of the AC admittance is changing the effective inductance of the LC resonator, leading to a frequency shift.

In the simplest possible case where there is only one conducting channel with some transparency as realized in atomic point contacts, a single spin-degenerated Andreev bound state appears. This leads to two Andreev levels at energies $-E_A(\varphi)$ and $+E_A(\varphi)$. These are fermionic degrees of freedom. Hence, each level is a doublet as long as there is no magnetic field and vanishing SOI.

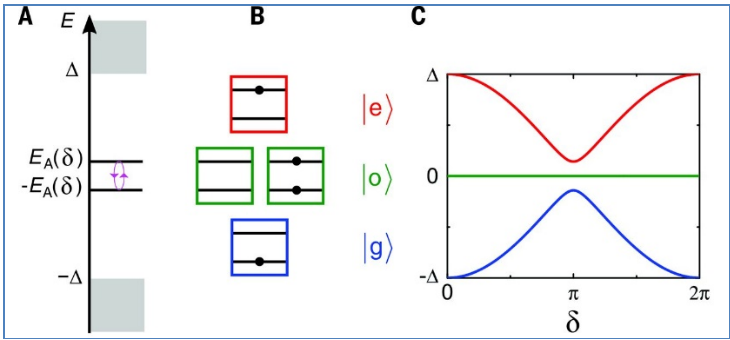

***Fig.4**. **Occupation of a Pair of Andreev levels** taken from Janvier et al. 5. Without SOI and without a Zeeman field there are three states, the even ground (blue) and excited (red) state, that show dispersion as a function of phase difference **δ**, and, hence, carry a supercurrent. This is in contrast to the two odd states, shown in green.*

In the ground state, the levels at negative energies are occupied. The pair of even states depicted in blue and red of Fig.4.B form the so-called **Andreev level qubit** in the even parity sector. In atomic-size contacts the odd sector is spin degenerated and hence cannot be addressed. The key question of task 4.1 is to implement a JJ where the spin degeneracy is lifted and where the spin degree of freedom can be addressed for qubit manipulation.

Within AndQC we make use of gate-tunable JJ made from semiconducting nanowires. Here, gate tuning allows controlling the number of participating transport channels and their transparencies. And, most importantly, the large SOI in InAs NWs allows addressing spins states via a charge degree of freedom. This has been theoretically analyzed, first, in the following paper [13] by the UAM team (also before this project started).

This work first points out that the Andreev bound states remain spin-degenerate in a single-channel weak linkwith Rashba SOI and at zero magnetic field. The paper shows that if two subbands of the semiconductor are close enough in energy, Rashba SOI and a phase bias with $\delta \neq 0 \bmod \pi$ lifts the spin degeneracy. -.[13] This is explained in Fig.5 taken from Park and Levy Yeyati.[13]

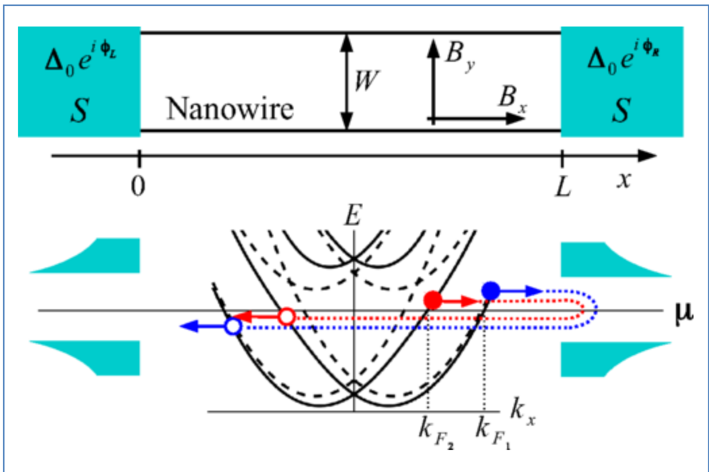

***Fig.5**. **Andreev Bound States in a Rashba Nanowire** taken from Park and Levy Yeyati.[13] The blue and the red electron states belonging to two different spin-states (effective spin states in Rashba NWs) result in two Andreev bound states (ABSs) when being Andreev reflected at the source and drain side. The two ABSs are degenerate in a single mode Rashba wire since the Fermi velocity is independent of the spin state. The effective admixture from a second mode changes the Fermi velocity for the two states and therefore lifts the spin degeneracy.*

In the vicinity of phase bias $\delta = \pi$ the dispersion of the Andreev levels is shown in Fig.6. The theory predicts that the two odd states have different supercurrents for the two spin states. Hence, they can be distinguished in superconducting circuits.

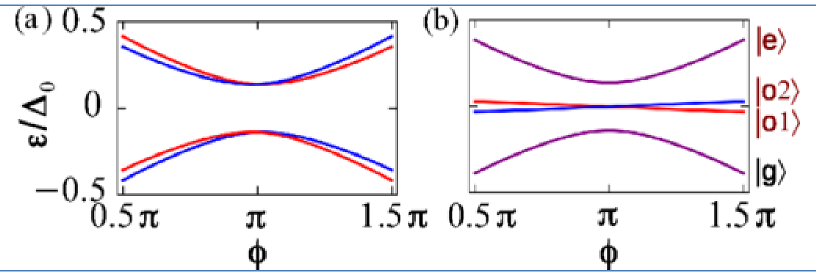

Fig. 6: Spin-lifted Andreev States *taken from Park and Levy Yeyati (UAM).[13] The two blue and red doublets from Fig.4 are lifted in a multimode Rashba NW for $\boldsymbol{\delta \neq 0}$ mod $\boldsymbol{\pi}$ even without a magnetic field. The red and blue dispersions now belong to the two "pseudospin" states. Note that $\boldsymbol{\varepsilon(-\delta) = -\varepsilon(\delta) holds\ if\ B = 0}$. (b) shows the total energy in the occupation number picture. For the even ground state $|\boldsymbol{g}\rangle$ both the blue and red negative energy states are occupied (seen on the left). Similarly, for the even excited state $|\boldsymbol{e}\rangle$ both the red and blue states at positive energy are occupied. In the odd states $|\boldsymbol{o1}\rangle, |\boldsymbol{o2}\rangle$, there is only one excitation. In this drawing either the red pair or the blue pairs in (a) make up a total energy state in (b). The red one has negative dispersion, while the blue one a positive.*

This proposal has been confirmed in a milestone paper entitled "*Spin-Orbit Splitting of Andreev States Revealed by Microwave Spectroscopy"* by L. Tosi *et al.* [7], a collaborative effort between CEA, UAM and UCPH. This work was writtenduring the preparation and submission phase of the AndQC project.

The main experimental finding is summarized in Fig.7 adapted from the L. Tosi *et al.* paper.

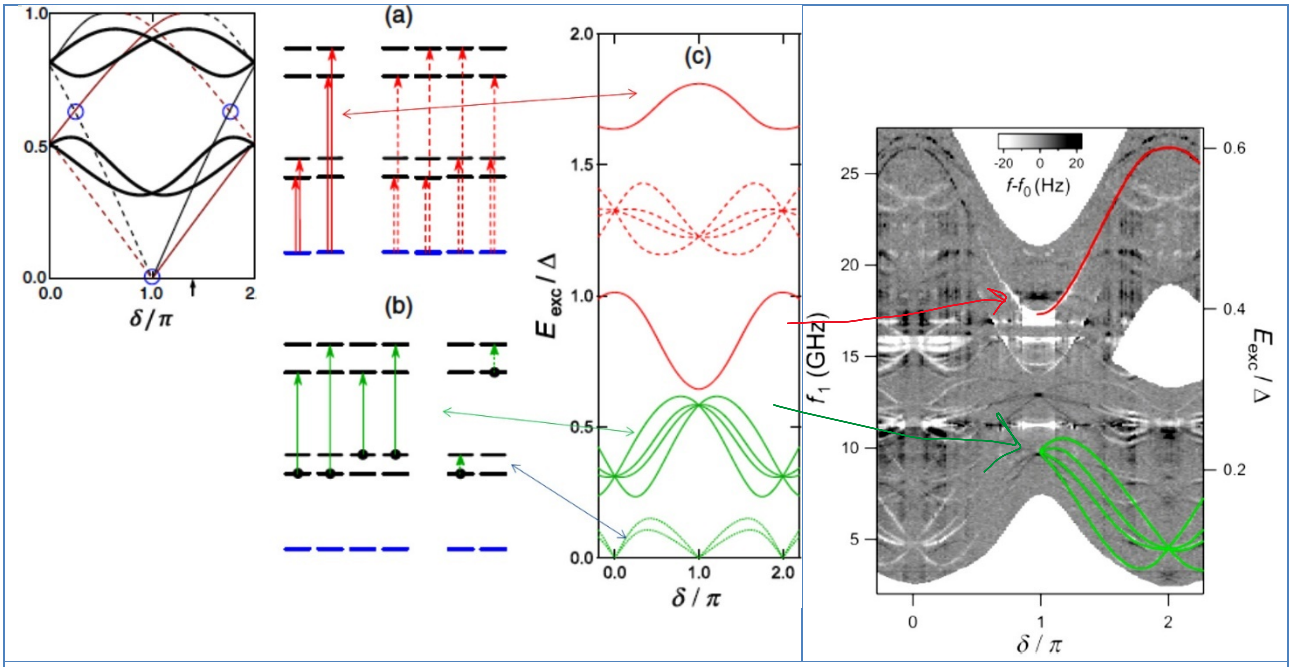

Fig. 7: Experimental Verification of Spin-Split Andreev States *taken from by L. Tosi et al. [7]. The figure on the right shows two-tone spectroscopy obtained for an InAs NW JJ tuned by the DC gate voltage to a situation where both pair and single electron excitation due to (at least) two mode NW can be discerned. The assignment with Andreev bound states is shown in the schematics on the left side.*

In the experiment bundles of four transition lines degenerate at $\delta = 0$ and $\delta = \pi$ have been observed. They are highlighted in the measurement and schematics by the green solid curves. They correspond to spin-conserving and spin-non-conserving transitions between Andreev levels belonging to different manifolds. These two manifolds are shown in the leftmost graph by pairs of black solid curves. In more recent experiments by the CEA team, transitions within a manifold were evidenced [8] . However, the states with opposite spins could not be discriminated in a single shot.

The CEA team also explored the dependence of the four "green" single electron excitations close to $\delta = \pi$ in a weak magnetic field. It was shown that the degeneracy at $\delta = \pi$ is lifted in a way that depends on the orientation of the magnetic field. If the field is applied parallel to the NW the even symmetry is maintained, while an asymmetry appears for a perpendicular field.[7]

In the follow-up work by the CEA and UAM team, a quantitative theory for the (positive and negative) shifts of the resonator frequency in two-tone spectroscopy has been developed. This work together with new experiments were published in Jan. 2021: C. Metzger *et al.* [8] It is based on a previous publication by Park *et al.*[14] Here, using the Bogoliubov-de Gennes formalism to describe the JJ, the shift of the resonator frequency as a function of level occupancy has been derived. This general theory [14] also interpolates between the adiabatic regime, where f_r is far detuned from possible excitations, and the Jaynes-Cumming regime for which virtual transitions between excitations that are not too far from f_r have an appreciable effect on the observed shift δf_r of the loaded resonator frequency.

In these new experiments also longer Josephson NW junctions were considered. The larger length leads to a larger dipole moment which couples with the asymmetric gate field used to drive transitions. In addition to this, the inductive coupling of the RF-SQUID to the resonator was maximized by a direct galvanic coupling of the resonator short at the end of the $\lambda/4$ resonator and one arm of the RF-SQUID loop. Both measures increased the coupling strength considerably. An example taken from this work is shown in Fig. 8.

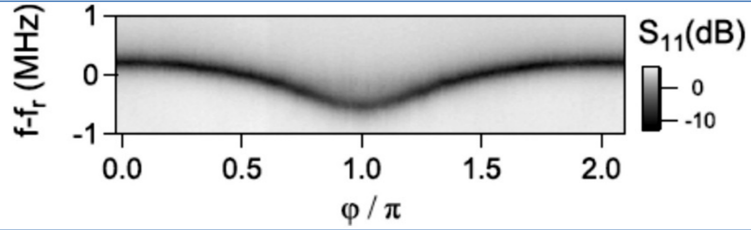

***Fig.8**. **Frequency Shift of a "Longer" InAs NW JJ** taken from Metzger et al.* [8]*. Note, that the frequency shift increased from 10Hz to up to 1MHz, i.e. by up to five orders of magnitude!*

The general formalism for the frequency shift of the loaded resonator when (only) state (i,σ) is occupied (i counts for the ABS and σ for the spin), yields two contributions:

a) the *adiabatic part* given by

$$E''_{i\sigma} + \sum_{j\sigma' \neq i\sigma} \mathcal{M}^2_{i\sigma,j\sigma'} \left(\frac{2}{E_{i\sigma,j\sigma'}} \right)$$

where the first part is the "curvature", that corresponds to the inverse (zero-frequency) inductance of the JJ and

b) the *dispersive part* (Jaynes-Cumming part) that involves virtual transition between state (i,σ) and (j,σ') and back to (i,σ) including resonator photon absorption or emission (see left).

$$\sum_{j\sigma' \neq i\sigma} \mathcal{M}^2_{i\sigma,j\sigma'} \left(-\frac{1}{E_{i\sigma,j\sigma'} - hf_r} - \frac{1}{E_{i\sigma,j\sigma'} + hf_r} \right)$$

This is illustrated in the paper by first looking into the reference JJ, which is a single-atom Al junctions, tuned to a single channel with low transmission (seeFig.9). On the left side we see that the sign and amplitude of the resonator frequency shift qualitatively follows the "curvature", i.e. the first term of the adiabatic part. The shifts are (not unexpectedly) much larger when the excitation frequency crosses the resonator frequency. In its vicinity virtual resonator transitions need to be considered. These theoretical results coincide with those obtained from a linear response derivation of the admittance of a weak-link in the short junction limit.[15]

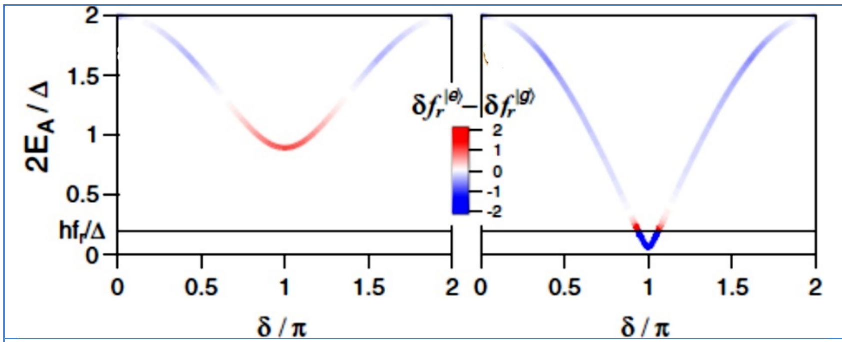

***Fig. 9: Resonator Response of a Single Andreev Level as a Function of Phase Bias** taken from Metzger et al.* [8]*. There is only one channel, and the JJ is probed when driving transitions from the even ground state to the even excited state. In the example on the left side, the resonator frequency* f_r *is far detuned from the excitation energy (single-atom contact with lower transmission), while on the right example the excitation frequency even crosses the resonator frequency.*

For longer JJs made with the InAs NWs, the complexity increases, due to many more possible transitions. Revealing is the question under what conditions one may encounter only spin-conserving or also spin non-conserving transitions in two-tone spectroscopy. For these junctions both interband and intraband spin-flip transitions could be found. This, even in the absence of a Zeeman field. The intraband spin-flip transitions were not seen in the previous work by L. Tosi *et al.* [7] . That they can be seen now is a milestone for this project, since it means that it is not only possible to define an Andreev spin qubit, for example in the lowest Andreev level manifold, in state $|1,\uparrow\rangle$ and $|1,\downarrow\rangle$, but one can also manipulate the state using microwave fields. The two states can be split by a phase bias and transitions can be induced by a resonant RF field applied to the gate electrode of the NW. This should induce Rabi oscillation between the spin up and spin down states.[16]

Figure 10 shows the predication for the case of a longer JJ with more than one transport channel. The JJ is assumed to have cylindrical symmetry, but the gate potential can be applied as an even function with respect to *y*, or with an asymmetric potential (see (a) in Fig.9).

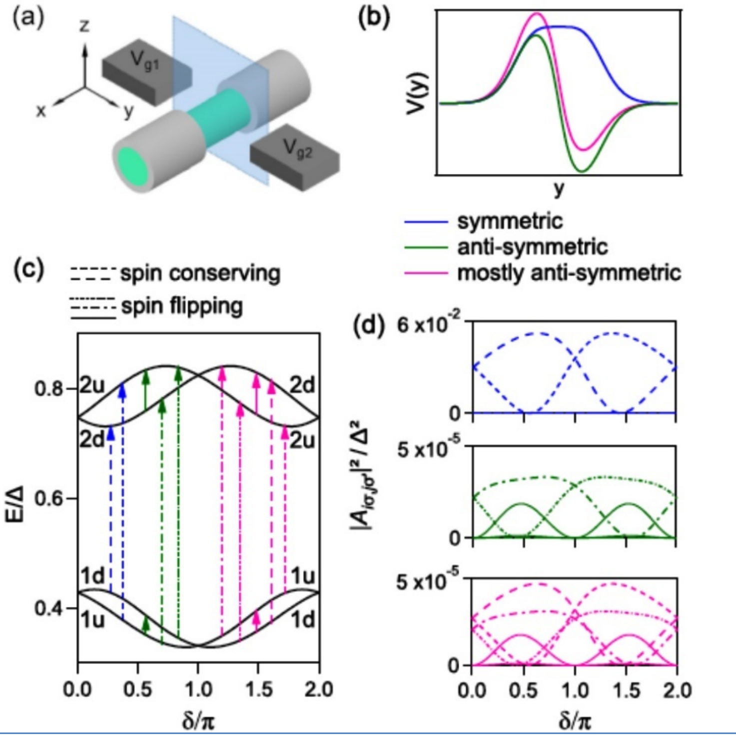

***Fig. 10: Theoretical Resonator Response of a "longer" InAs NW JJ as a Function of Phase Bias** taken from Metzger et al.* [8]

The illustration shows in blue that only spin-conserving transitions are allowed if the gate potential is symmetric. In the fully asymmetric case, shown in green, only spin-non-conserving transitions are allowed. In general, both transitions could be seen. This should give rise to two low energy branches (intraband spin-flip transitions) and four higher energy branches (interband transitions).

The next and final figure shows one representing experimental result for such a longer InAs NW JJ.

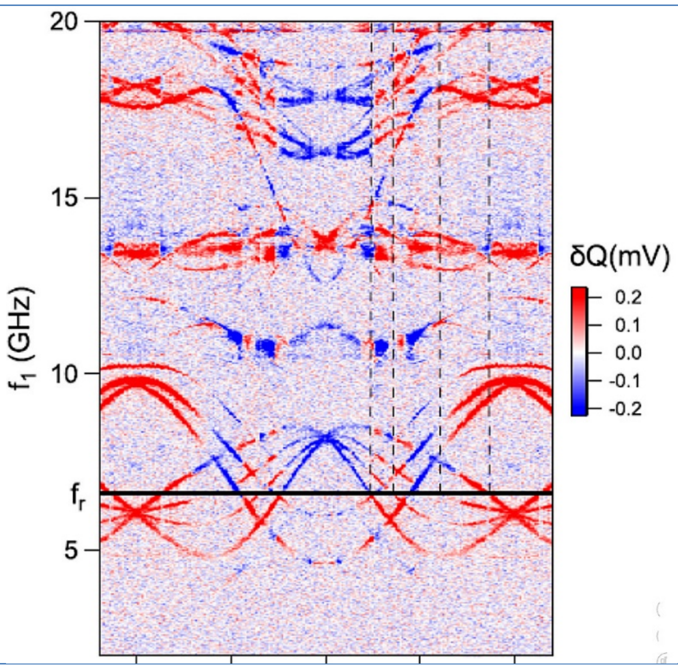

***Fig. 11: Experimental Resonator Response of a "longer" InAs NW JJ as a Function of Phase Bias** taken from Metzger et al.* [8]

Two-tone spectrum measured on an InAs NW JJ of length L ~ 550 nm and using a resonator at $\boldsymbol{f_r = 6.6}$ GHz. The color-coded quadrature of the measured signal shows many sign changes along the transition lines, qualitatively in agreement with the behavior illustrated in Fig.9.: the sign changes are attributed to situations where the energy of some virtual transitions match $\boldsymbol{f_r}$.

There has been further work done at CEA, UBAS, and Chalmers. In particular, it was shown in a collaborative effort between Yale, Chalmers, and UCPH, that the resonator allows to distinguish the different states in a single-shot readout resonator tone, applied during $1.9\ \mu s$ with a fidelity of 92%.[17] Further, the ASQ transition in the lowest energy branch could also be driven by a Raman transition in a coherent way.[16] The coherent manipulation is, however, beyond deliverable D4.1. It will be discussed later in D4.2 and 4.3.

3. Summary / Conclusion

It has been shown that in "long" JJs with more than one mode, the spin-states can be lifted solely by an applied phase bias $\delta \neq 0 \ mod \ \pi$. The lowest energy state $|1\rangle$ could be used to define a spin qubit in the states $|1 \uparrow\rangle$ and $|1 \downarrow\rangle$. This odd state may have a lifetime up to ms and spin relaxation times in the range of $50\mu s$ have been demonstrated. First studies show coherence times in the tens of ns.[16] Further studies will focus on state manipulation, possibly also with other wires that do not have a strongly dephasing nuclear bath. The purpose of this task, namely to *"map this spin-dependent transitions in the presence of a weak magnetic field, spin-orbit coupling and multiple propagating modes"* has been achieved in full.

4. Literature

1. L. Bretheau, C. O. Girit, H. Pothier, D. Esteve and C. Urbina, Nature **499** (7458), 312-315 (2013).
2. L. Bretheau, C. O. Girit, C. Urbina, D. Esteve and H. Pothier, Physical Review X **3** (4), 041034 (2013).
3. L. Bretheau, C. O. Girit, M. Houzet, H. Pothier, D. Esteve and C. Urbina, Phys. Rev. B **90** (13), 134506 (2014).
4. C. Janvier, L. Tosi, C. O. Girit, M. F. Goffman, H. Pothier and C. Urbina, Journal of Physics-Condensed Matter **26** (47), 474208 (2014).
5. C. Janvier, L. Tosi, L. Bretheau, C. O. Girit, M. Stern, P. Bertet, P. Joyez, D. Vion, D. Esteve, M. F. Goffman, H. Pothier and C. Urbina, Science **349** (6253), 1199-1202 (2015).
6. R. Haller, G. Fülöp, D. Indolese, J. Ridderbos, R. Kraft, L. Y. Cheung, J. H. Ungerer, K. Watanabe, T. Taniguchi, D. Beckmann, R. Danneau, P. Virtanen and C. Schönenberger, arXiv:2108.00989 (2021).
7. L. Tosi, C. Metzger, M. F. Goffman, C. Urbina, H. Pothier, S. Park, A. L. Yeyati, J. Nygard and P. Krogstrup, Physical Review X **9** (1), 011010 (2019).
8. C. Metzger, S. Park, L. Tosi, C. Janvier, A. A. Reynoso, M. F. Goffman, C. Urbina, A. L. Yeyati and H. Pothier, Physical Review Research **3** (1), 013036 (2021).
9. M. F. Goffman, R. Cron, A. L. Yeyati, P. Joyez, M. H. Devoret, D. Esteve and C. Urbina, Phys. Rev. Lett. **85** (1), 170-173 (2000).
10. P. Virtanen, F. S. Bergeret, J. C. Cuevas and T. T. Heikkila, Phys. Rev. B **83** (14), 144514 (2011).
11. F. Kos, S. E. Nigg and L. I. Glazman, Phys. Rev. B **87** (17), 174521 (2013).
12. M. Ferrier, B. Dassonneville, S. Gueron and H. Bouchiat, Phys. Rev. B **88** (17), 174505 (2013).
13. S. Park and A. L. Yeyati, Phys. Rev. B **96** (12), 125416 (2017).
14. S. H. Park, C. Metzger, L. Tosi, M. F. Goffman, C. Urbina, H. Pothier and A. L. Yeyati, Phys. Rev. Lett. **125** (7), 077701 (2020).
15. P. D. Kurilovich, V. D. Kurilovich, V. Fatemi, M. H. Devoret and L. I. Glazman, arXiv:2106.00028 (2021).
16. M. Hays, V. Fatemi, D. Bouman, J. Cerrillo, S. Diamond, K. Serniak, T. Connolly, P. Krogstrup, J. Nygard, A. L. Yeyati, A. Geresdi and M. H. Devoret, Science **373** (6553), 430 (2021).
17. M. Hays, V. Fatemi, K. Serniak, D. Bouman, S. Diamond, G. de Lange, P. Krogstrup, J. Nygard, A. Geresdi and M. H. Devoret, Nat. Phys. **16** (11), 1103 (2020).